Arabian Journal of Geosciences (2021) 14: 1515
https://doi.org/10.1007/s12517-021-07851-4

ORIGINAL PAPER

Heterogeneity of tight sandstone reservoirs based on fractal theory: the Xu-6 member of Xujiahe Formation in Guang'an area, central Sichuan Basin

Fang Shen[1,2] · Liang Yue[3] · Ziliang Liu[1,2] · Wei Yang[4] · Kaarel Mänd[5] · Hui Jin[4] · Fengjie Li[1] · Yue Zhou[1,2] · Minghe Zhang[1,2] · Rui Jiang[1,2]

Received: 16 April 2021 / Accepted: 23 June 2021 / Published online: 27 July 2021

Abstract

The clastic rocks of the late Triassic Xujiahe Formation in the Sichuan Basin of southwestern China are typical unconventional tight sandstone reservoirs with proven natural gas reserves of up to one trillion cubic meters. In particular, the Xu-6 member of the Xujiahe Formation in the Guang'an area of the central Sichuan Basin is a gas reservoir with great exploration and development potential. In this study, we studied the petrography, measured the geophysical properties, and performed mercury injection tests and calculations based on fractal theory on a suite of tight gas sandstone samples from the Xu-6 member to evaluate the pore types and volumes, permeability, and heterogeneity of the reservoirs. The results show that the sandstone reservoirs of the Xu-6 member of the Xujiahe Formation can be divided into the following three types. Type I reservoirs, which are generally of high quality (an average porosity of 12.59% and an average permeability coefficient of 6.8231×10^{-3} μm^2), are dominated by macroscale pores and a uniform distribution of mesoscale and microscale pores; the fractal dimension is 2.45 to 2.59. Type II reservoirs (an average porosity of 8.9% and an average permeability coefficient of 1.3504×10^{-3} μm^2) are dominated by mesoscale pores, followed by microscale pores, whereas the macroscale pores are poorly developed; the fractal dimension range is 2.42–2.69. Type III reservoirs, typically of low quality (an average porosity of 4.67% and an average permeability coefficient of 0.2947×10^{-3} μm^2), are dominated by microscale pores, followed by mesoscale pores with poorly developed or undeveloped macroscale pores; the fractal dimension is 2.46 to 2.81. The varying distribution of pore types leads to significant differences in pore heterogeneity for the three types of reservoirs, suggesting that type III reservoirs are more heterogeneous than type I reservoirs. Our correlation analysis reveals that the physical properties are related to the reservoir heterogeneity, as proxied by the fractal dimension. When the fractal dimension is between 2.45 and 2.6, porosity is variable, but generally high, whereas permeability shows no obvious relationship to the fractal dimension. When the fractal dimension is greater than 2.6, there is a decreasing trend in porosity, and permeability remains at a constant low value as the fractal dimension increases. Based on our quantitative study of physical properties and fractal characteristics of the Xu-6 member sandstone reservoir, microscopic pore characteristics such as fractal dimension hold great theoretical and practical significance as evaluation criteria for unconventional high-quality natural gas reservoirs and can potentially be used for guiding their exploration and development.

Keywords Sichuan Basin · Guang'an area · Xujiahe Formation · Reservoir · Fractal dimension · Physical property conditions

Responsible Editor: Santanu Banerjee

✉ Ziliang Liu
bugliu2001@163.com

[1] State Key Laboratory of Oil and Gas Reservoir Geology and Exploitation, Chengdu University of Technology, Chengdu 610059, Sichuan, China

[2] College of Energy, Chengdu University of Technology, Chengdu 610059, Sichuan, China

[3] Jiangsu Vocational Institute of Architectural Technology, Xuzhou 221116, Jiangsu, China

[4] PetroChina Research Institute of Petroleum Exploration & Development, Beijing 100083, China

[5] Department of Geology, University of Tartu, 50114 Tartu, Estonia

Introduction

Unconventional natural gas exploration has greatly changed the pattern of energy supply worldwide, yet it is currently only in its initial development stage (Law and Curtis 2002; Hou et al. 2015). The Xujiahe Formation gas reservoir in central Sichuan forms a typical tight sandstone gas reservoir with low porosity and permeability, which is characterized by a "large area, low abundance, and local enrichment" (Schmoker 2002; Zou et al. 2009). Nonuniform continuous sand bodies with low porosities and permeabilities are dominated by lithologic traps, resulting in ambiguous trap shapes and boundaries. The complex formation mechanisms and the dynamic balance of the diagenetic traps in tight sandstone gas reservoirs pose challenges to accurate predictions of gas potential (Zou et al. 2013).

Previous studies on the tight sandstone reservoir in the Xujiahe Formation have mostly focused on the characteristics and variations in sedimentary facies in the reservoir strata, the associated mineral compositions and secondary alterations (Lai et al. 2018b; Zhang et al. 2019), the pore types and their distributions (Zhu HH et al. 2014; Huang et al. 2016), and the classification of different diagenesis stages (Zeng 2010; Chen et al. 2014). However, after the launch of gas production from continuous gas reservoirs, many problems such as an unstable and rapidly decreasing natural gas supply, have been encountered, which have severely limited the economic benefits. Regarding the factors controlling the physical properties of the Xu-6 Formation reservoir strata and the decrease in gas production, scholars have discussed the influences of the sedimentary environment and the evolving diagenesis process (Zhu T et al. 2014; Gu 2017), the gas-water distribution (Li et al. 2017; Luo et al. 2016), and the effect of gas seepage under a pressure gradient (Fu et al. 2010). Under the dominant mechanism of compaction (Lundegard 1992), porosity usually decreases with increasing depth (Paxton et al. 2002; Ehrenberg et al. 2009) and the enhanced pressure at greater depth promotes the physical compaction of clastic sediments and produces mineral chemical reactions (Ehrenberg and Nadeau 2005; Taylor et al. 2010; Albrecht and Reitenbach 2015), both of which lead to an increased complexity in the physical properties of reservoir strata. These physical properties, especially pore structure, represent a key index for assessing the storage effectiveness and the reservoir formation probability in unconventional reservoir strata.

Since its establishment, fractal geometry has been widely applied to characterize the microscopic pore structure of rocks (Zhu et al. 2018). This method can precisely and quantitatively describe the complexity of the pore structure of nonconventional reservoir strata and can thus be used to determine and assess "sweet spots" for tight gas reservoirs. Currently, a fractal theory approach based on mercury injection test data is the most common and sophisticated method (Huang et al. 2017) and has been widely applied in the study of tight sandstones (Lai et al. 2015, b; Zhu et al. 2019). However, previous studies of the fractal characteristics of the Xujiahe Formation have mostly focused on shale gas reservoirs (Huang et al. 2016; Deng et al. 2018), with very little work on tight sandstone reservoir strata.

The Xu-6 member of the Xujiahe Formation in the Guang'an gas field is a typical lithologic gas reservoir that possesses a high industrial production capability. Currently, the detected reservoir amount is 788×10^8 m^3 (Zhao et al. 2010). The macroscopic characteristics of the Xu-6 reservoir stratum are represented by large horizontal variations and strong heterogeneities, while the microscopic characteristics are dominated by poorly developed fractures, a low porosity, and a low permeability. In this study, we conducted mercury injection tests, microscope observations, statistical analysis of rock samples, log analysis, and calculations according to fractal theory. Based on the results, we assessed the physical properties of tight sandstone gas reservoir strata of the Xu-6 member in the Guang'an gas field well 101. We also quantitatively investigated the correlations between the physical properties, pore structure, and fractal dimension of gas storage sandstones, classified the reservoir strata into different types based on pore structure, and discussed the general physical characteristics of premier tight sandstone reservoir strata to provide a geological basis for the exploitation and development of this type of tight gas in the Guang'an area.

Geological background

Guang'an, which is located in the central and eastern parts of the Sichuan Basin, experienced the full sedimentary evolution and tectonic movement history of the Sichuan Basin (Tong 2000; Zheng et al. 2009; Shi et al. 2012). In the Lower to Middle Triassic (and earlier), marine facies strata mainly carbonates were deposited. The Upper Triassic to Paleogene saw the deposition of lacustrine facies strata, mainly composed of sandstones and mudstones. The area experienced multiple tectonic episodes including the Caledonian Movement, the Hercynian Movement, the Indochina Movement, the Yanshan Movement, and the Himalayan Movement (Tong 2000; Zheng et al. 2009; Shi et al. 2012). The Guang'an tectonic anticline is located to the east of the oblique and gentle Gulongzhong structural zone in central Sichuan, whereas the Guang'an gas field is located to the east of the Guang'an tectonic anticline (Fig 1).

The Upper Triassic Xujiahe Formation in central Sichuan can be divided into six members, of which the Xu-1, Xu-3, and Xu-5 members are limnetic deposits that largely consist of black shales and siltstones and the Xu-2, Xu-4, and Xu-6 members are delta-plain-delta-front deposits that mainly consist of feldspar clastic sandstones, clastic sandstones, and

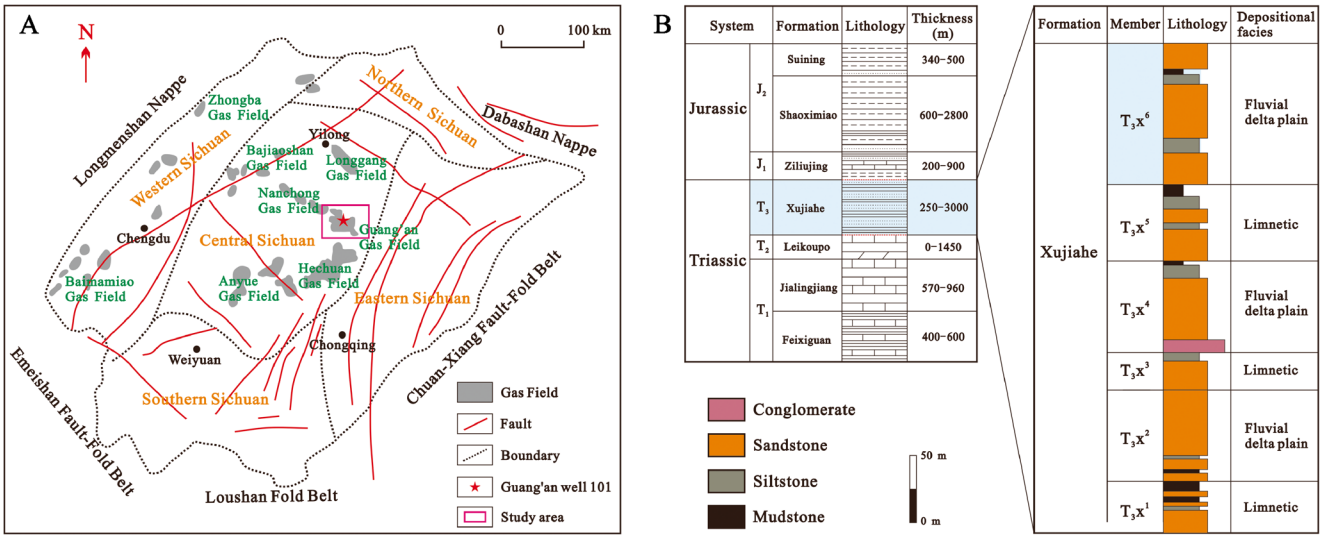

Fig. 1 **A** Gas field distribution in the Sichuan Basin and **B** stratigraphic column of the Xujiahe Formation (modified from Tong 2000; Wang et al. 2013; Yu et al. 2014)

feldspar sandstones (Zheng et al. 2009; Lai et al. 2018a). Some scholars have proposed that the Xujiahe Formation represents a tide delta deposit (Zhao XF et al. 2019). The Xu-6 member in Guang'an, in particular, is a braided river delta-lake deposit that is mainly composed of medium-to-coarse-grained feldspar clastic sandstones and clastic sandstones, which are intermixed with thin layers of shales, plant-containing clastic sandstones, siltstones, and coaling lines. The top of the Xu-6 member is a limnetic deposit consisting of mudstones embedded with coals that pseudoconformably underlies the early Jurassic quartz siltstones in the Zhenzhuchong Formation.

Methods

Sampling location and measurements

Multiple analytical methods have been applied to quantitatively study pore structures, including scanning electron microscopy (SEM), transmission electron microscopy (TEM), micro computed tomography (micro-CT), small-angle neutron scattering, and molecular adsorption. However, due to the limitations of these methods and the heterogeneous features of samples, the adoption of a single analytical method in a limited observational scale cannot fully capture the overall characteristics of a reservoir stratum. Instead, different techniques can be utilized to yield multiple assessment results (Zou et al. 2015).

In this study, we obtained 54 sandstone samples from the gas reservoir section (2025–2095 m) of the Guang'an gas field well 101 (Fig. 2). We conducted thin section observations and mercury injection tests to determine the physical properties of the samples and to determine the distribution of pores using fractal calculations. Thin sections were observed using polarizing light microscopy and electron microscopy, the latter using a ZEISS SIGMA300 scanning electron microscope. For mercury injection analyses, the sandstone samples were processed to plungers with a diameter of 2.5 cm. The samples were first dried for 2.5 h, and the mercury injections were then carried out using a fully automated AutoPore IV mercury injection instrument; the measured pores ranged in size from 0.003 to 1000 μm.

Fractal dimension calculations

Fractal theory can be effectively applied to study irregular bodies with complex structures and self-similarity; hence, it has been widely adopted to describe reservoir stratum characteristics. The value of the fractal dimension D is usually between 2 and 3: the case of $D = 2$ represents a homogeneous pore structure, and the case of $D = 3$ represents a heterogeneous pore structure. We adopted the high-pressure mercury injection curve to calculate the fractal dimension D for the tight reservoir strata, the derivation of which is as follows (Feng and Zhu 2019):

$$\mathrm{N}(>r) = \int_r^{r_m} P(r)dr = ar^D \tag{1}$$

where r is the pore radius (μm), $N(>r)$ is the number of pore throats with pore radii greater than r, r_m is the maximum radius (μm), $P(r)$ is the density distribution function of the pore radius, a is a constant ($a = 1$ represents tubular pores, and $a = 4\pi/3$ represents spherical pores), and D is the fractal dimension.

By taking the derivative of Equation (1), we obtain:

$$\mathrm{P(r)} = \frac{dN(>r)}{dr} = a'r^{-D-1} \tag{2}$$

where $a' = -D \times a$ is a constant.

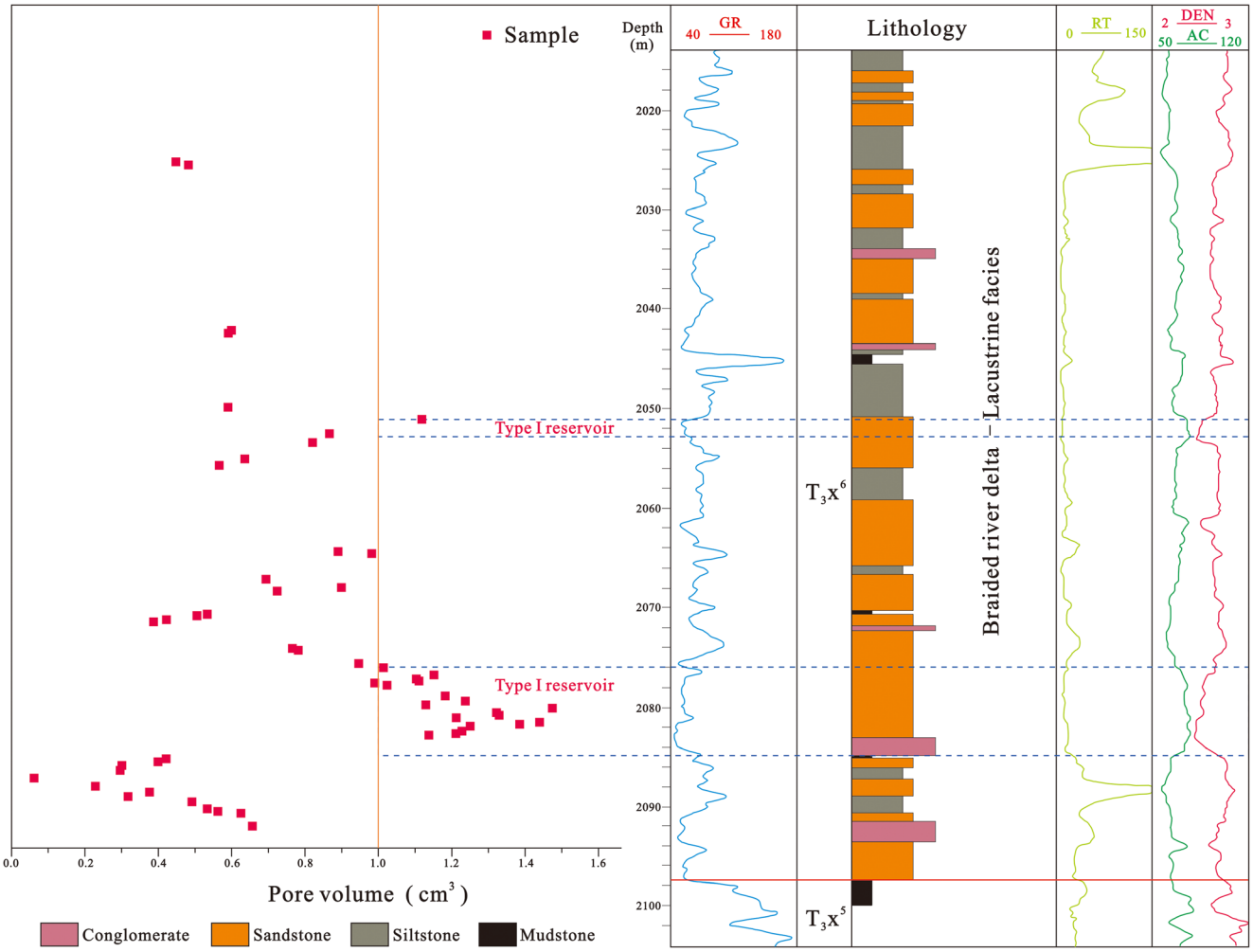

Fig. 2 Comprehensive stratigraphic column of Guang'an well 101, corresponding pore volumes calculated from mercury injection experiments ($n = 54$) and well log data. Abbreviations: GR gamma, RT resistivity, DEN density, AC acoustic slowness

By converting Equation (2) to Equation (3), we can obtain the total volume of pores with radii smaller than r, $V(<r)$:

$$\mathrm{V}(<\mathrm{r}) = \int_{r_s}^{r} P(r) a r^3 dr = a''\left(r^{3-D} - r_s^{3-D}\right) \tag{3}$$

where a" is a constant, $a'' = a' \times a/(3-D)$, and r_s is the minimum pore radius (μm).

The total pore volume of a tight sandstone reservoir stratum (V) can be expressed as follows:

$$\mathrm{V} = \mathrm{a}''\left(r_m^{3-D} - r_s^{3-D}\right) \tag{4}$$

By converting Equations (3) and (4) to Equation (5), we can calculate the proportion of the accumulated volume of pores with radii smaller than r:

$$f = \frac{V(<r)}{V} = \frac{r^{3-D} - r_s^{3-D}}{r_m^{3-D} - r_s^{3-D}} \tag{5}$$

where f is the proportion of the accumulated volume of pores with radii smaller than r.

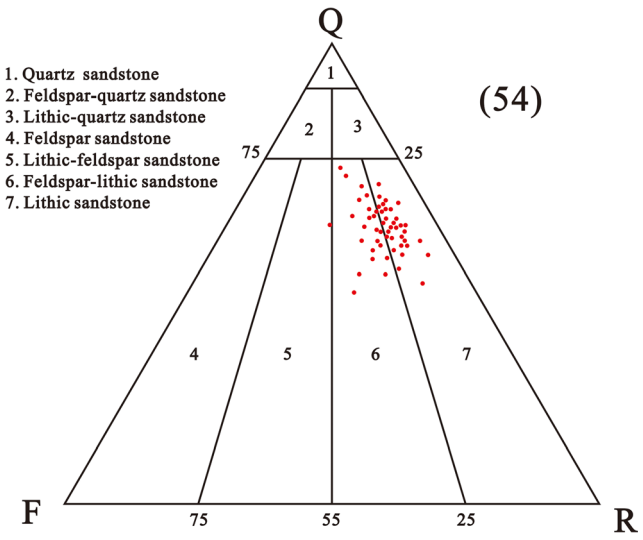

Fig. 3 Ternary QFR diagram of the matrix compositions of the Guang'an well 101 sandstones. Abbreviations: Q quartz, F feldspar, R rock fragments

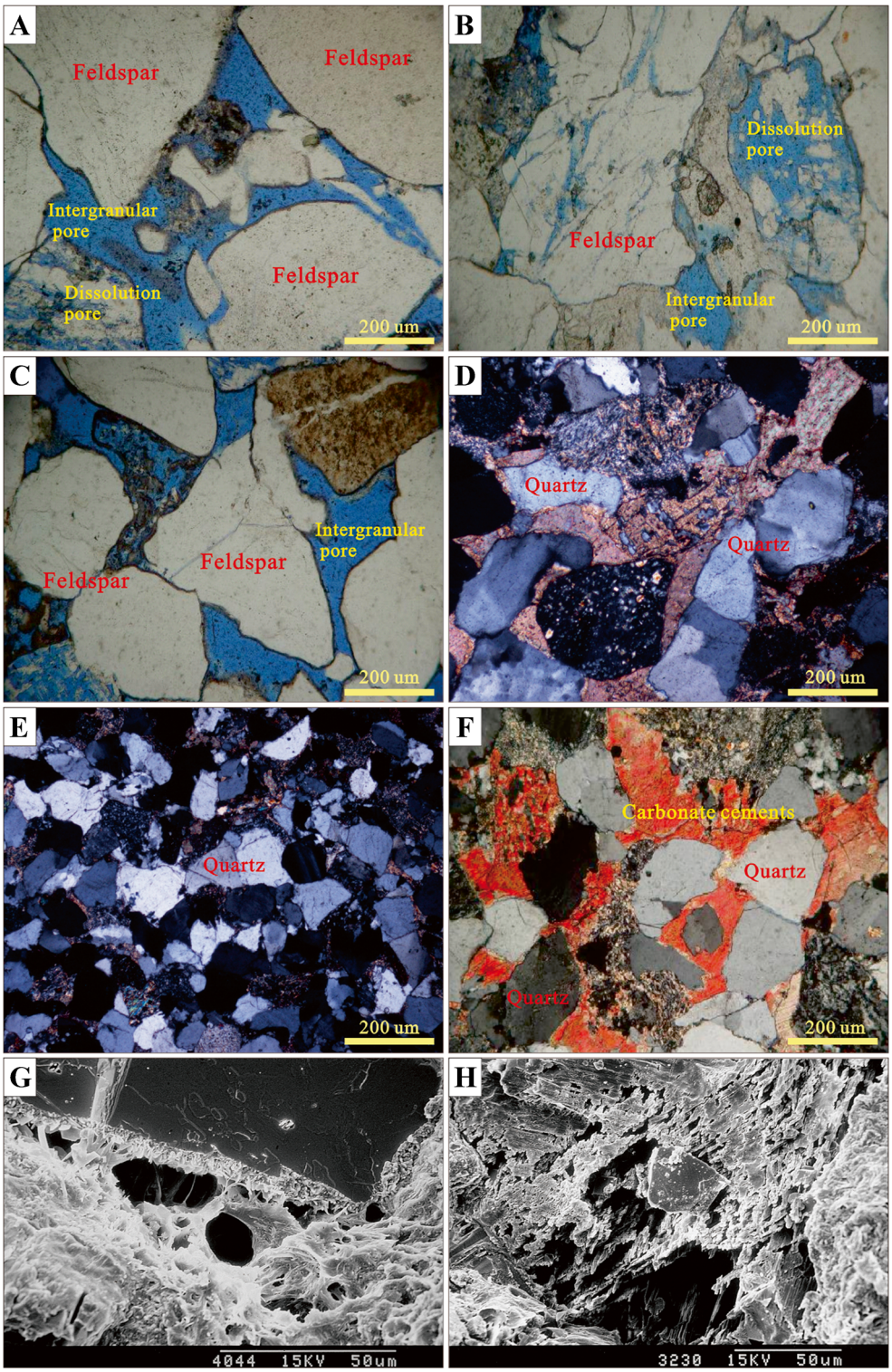

Fig. 4 Microscopic characteristics of sandstones in the Xu-6 member of the Xujiahe Formation. **A**–**C** Feldspathic lithic sandstone thin sections seen in single-polarized light. Primary intergranular pores and feldspar dissolution pores can be observed. **D**–**E** Lithic sandstone thin sections seen in cross-polarized light. The sandstones are grain- and matrix-supported. Secondary enlargement of quartz and poorly developed pores can be observed. **F** Lithic sandstone thin sections seen in cross-polarized light. Carbonate cement fillings and poorly developed pores can be seen. **G** Scanning electron micrograph (secondary electron) of illite with intergranular pore fillings, development of chlorite films, and well-developed pores. **H** Scanning electron micrograph of dissolved feldspar grains that resulted in the formation of intragranular pores

In this study, assuming that the minimum pore radius r_s is much smaller than the maximum pore radius r_m, we can further simplify Equation (5) to:

$$f = \left(\frac{r}{r_m}\right)^{3-D} \tag{6}$$

By applying the Young-Laplace equation, the mathematical relationship between the capillary pressure and the pore radius can be expressed as:

$$P_c = \frac{2\sigma\cos\theta}{r} \tag{7}$$

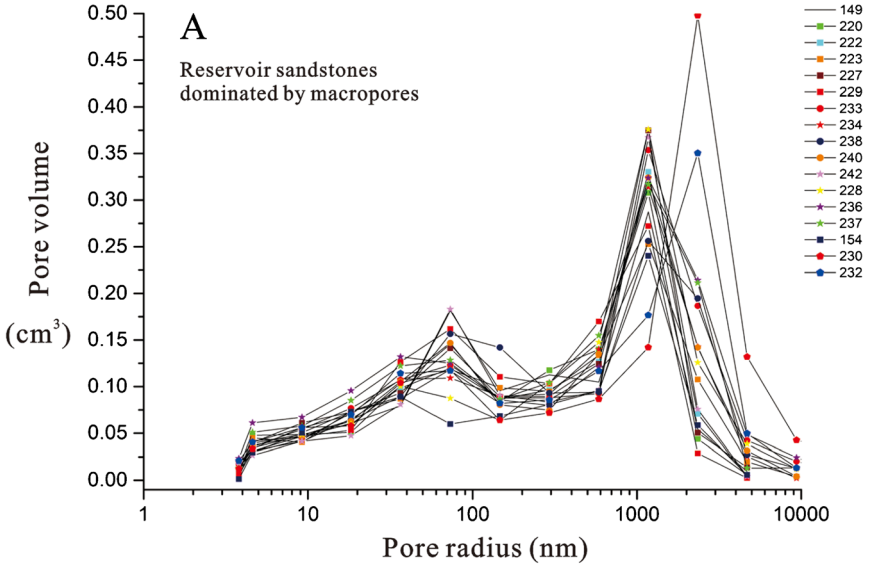
A
Reservoir sandstones
dominated by macropores
Pore volume
(cm³)
Pore radius (nm)
149
220
222
223
227
229
233
234
238
240
242
228
236
237
154
230
232

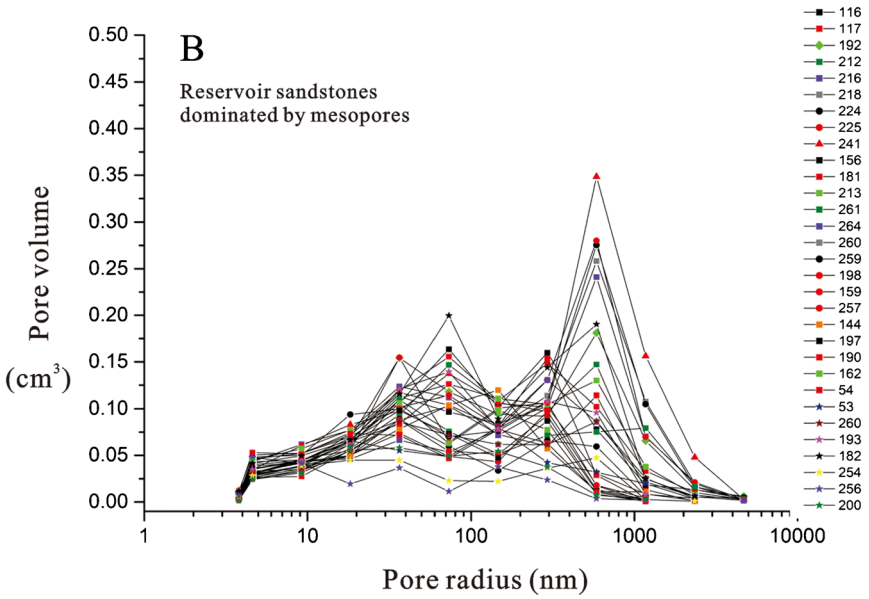
B
Reservoir sandstones
dominated by mesopores
Pore volume
(cm³)
Pore radius (nm)
116
117
192
212
216
218
224
225
241
156
181
213
261
264
260
259
198
159
257
144
197
190
162
54
53
260
193
182
254
256
200

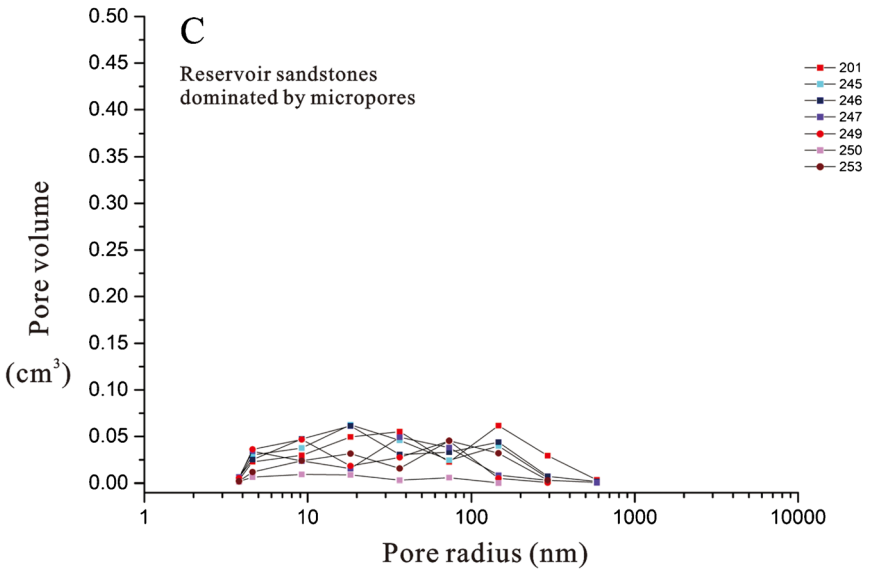
C
Reservoir sandstones
dominated by micropores
Pore volume
(cm³)
Pore radius (nm)
201
245
246
247
249
250
253

◀ **Fig. 5.** Cross plot of pore throat radii and volume in samples from the Xu-6 sandstone reservoirs, based on mercury injection data. **A** Reservoir sandstones dominated by macropores. **B** Reservoir sandstones dominated by mesopores. **C** Reservoir sandstones dominated by micropores

where P_c denotes the capillary pressure (MPa), θ is the wetting angle (°), and σ is the surface tension between air and mercury (N/m).

In this study, assuming that the wetting angle is unaffected by the pore radius, Equation (7) can be converted to:

$$S = \left(\frac{Pc}{Ps}\right)^{D-3} \tag{8}$$

where P_s is the mercury injection pressure (MPa) and S is the wetting-phase saturation. For high-pressure mercury injection experiments, $S = 1-S_{Hg}$ (S_{Hg} is the mercury injection saturation).

By taking the logarithm of Equation (8), we can convert it to Equation (9), which is the equation for calculating the fractal dimension based on the capillary curve.

$$\log_{10}\left(1-S_{Hg}\right) = (D-3)\log_{10}P_c - (D-3)\log_{10}P_s \tag{9}$$

Results

Petrographic characteristics

Thin section petrography was used to statistically assess the grain composition of the samples. The Xu-6 member is mainly composed of feldspar clastic sandstones and clastic sandstones (Figs. 3 and 4). Quartz accounts for 48–73% of the total volume, with a mean of 63.5%; the observed quartz grains are poorly rounded and show secondary enlargements. Feldspar accounts for 16–68% of the total volume, with a mean of 63.5%. The clastic rock fragments are dominated by metamorphic clasts, followed by sedimentary and volcanic clasts, and their corresponding average volumes are 12.23%, 6.9%, and 6.39%, respectively. Matrix accounts for 0–33% of the total volume, with a mean of 6.53%, and consists mainly of chlorite, illite, kaolinite, and organic matter. Cements within sandstones are dominantly composed of carbonate and siliceous material, followed by chlorite. The sandstones are mainly grain-supported, but occasionally matrix-supported. Grains are subangular to subcircular in shape, representing a medium-to-poor sorting degree.

Pore types and distribution characteristics

Our analyses of the thin sections show that the Xu-6 reservoir strata mainly host primary intergranular pores, intergranular dissolution pores, intramatrix dissolution pores, intragranular dissolution pores, and moldic pores (Fig. 4). In particular, the premier storage strata consist mainly of feldspar clastic sandstones that are dominated by primary intergranular pores and intragranular dissolution pores, while the storage strata with low porosities consist mainly of clastic sandstones with high matrix contents. Within the premier Xu-6 storage strata, intragranular dissolution pores are commonly formed by the dissolution of feldspar, and some of them connect with primitive intergranular pores to form larger pores.

Pores in tight sandstones are usually on the order of nanometers in size, and their pore throat radii are smaller than 2 μm (Nelson 2009). According to the pore radius distribution curve obtained from mercury injection data for the 54 Xu-6 gas reservoir samples, we were able to recognize macropores (pore throat radii > 1 μm), mesopores (0.1–1 μm), and micropores (< 0.1 μm). Based on these results, we calculated the pore throat radius-volume distribution (Fig. 5 and Table 1). Macropores range between 0 and 59.55% in relative volume, with a mean of 17.70%; mesopores range between 16.15 and 53.09% in volume, with a mean of 37.68%; and micropores range between 22.06 and 83.85% in volume, with a mean of 44.62%.

According to the distribution of different pore throat radii, the tight sandstones gas reservoir samples can be divided into three types: ones dominantly composed of macropores (Fig. 5A), ones dominated by mesopores (Fig. 5B), and ones dominated by micropores (Fig. 5C). More specifically, sandstones dominated by macro- and mesopores exhibit a bimodal distribution for their pore throat radii, with the major peak representing macro- and mesopores and a lesser one representing micropores. In comparison, the pore throat radius curve for sandstones dominated by micropores shows a uniform distribution in the ~ 0.005 to 0.2 μm range, with no obvious peaks. In addition, there is a wide range in the maximum mercury injection saturation among different samples, which ranges from 55.66 to 98.43%, with a mean of 89.69%. The mercury withdrawal efficiency varies between 7.39 and 54.77%, with a mean of 32.79% (Table 1).

Reservoir types

By considering both the mercury injection curve and the distribution characteristics of the pore throat radii, the tight sandstone reservoirs in the study area can be divided into three types (Fig. 6 and Table 1).

For type I reservoirs, the porosity is larger than 10%, the permeability is larger than 0.5×10^{-3} μm^2, the average maximum mercury injection saturation is 97.51%, and the average mercury withdrawal efficiency is 46.16% (Table 1). Type I reservoirs usually have beneficial physical properties for gas production: their average porosity and permeability are 12.27% and 6.0376×10^{-3} μm^2, respectively. The main types of rocks are medium-to-coarse grained feldspathic lithic

Table 1 Physical properties and fractal dimension of the Xu-6 Member sandstone in the Guang'an area

Reservoir Type	Quantity		Maximum mercury injection saturation (%)		Mercury withdrawal efficiency (%)		Macropores (%)		Mesopores (%)
Type I	20	Range	94.85~98.43	55.66~98.43	41.94~54.77	7.39~54.77	15.67~59.50	0~59.50	18.44~51.12
		Mean	97.51	89.69	46.16	32.79	39.09	17.71	32.27
Type II	7	Range	91.27~97.75		40.98~52.58		1.23~19.63		44.56~52.14
		Mean	95.97		45.92		10.41		48.56
Type III	27	Range	55.66~97.86		7.39~52.68		0~18.75		16.15~53.09
		Mean	82.27		36.19		3.78		38.88

Reservoir Type	Mesopores (%)	Micropores (%)	Porosity (%)		Permeability (10^{-3} μm^2)		Fractal dimension	
Type I	16.15~53.09	22.06~34.66	22.06~83.85	10.05~15.16	0.66-15.16	1.0295~19.3679	0.0394~19.3679	2.42~2.59	2.42~2.81
	37.68	28.64	44.60	12.27	8.34	6.0376	2.5614	2.52	2.58
Type II		34.38~47.45		8.07~9.93		0.1479~1.8335		2.47~2.56	
		41.03		9.26		1.1523		2.51	
Type III		38.11~83.85		0.66~7.83		0.0394~1.0919		2.45~2.81	
		57.35		5.20		0.3517		2.64	

sandstones and gravel-bearing sandstones. Chlorite rims, quartz enlargements, and extensive feldspar dissolution are also commonly observed. The abundance of minerals with strong mechanical strengths (e.g., quartz, feldspar) in this type of reservoir can protect rock porosity (Pittman and Larese 1991), thus leading to the formation of premier reservoirs. In contrast, an abundance of plastic minerals can adversely affect the quality of reservoirs (Pittman and Larese 1991). Type I reservoirs are dominated by macro- and mesopores, including primary intergranular pores and intragranular dissolution pores, and can be classified as high-quality reservoirs (Zou et al. 2012).

For type II reservoirs, the porosity is larger than 8%, the permeability is larger than 0.1×10^{-3} μm^2, the average maximum mercury injection saturation is 95.97%, and the average mercury withdrawal efficiency is 45.92% (Table 1). These types of reservoirs usually have good physical properties for gas production, and their average porosity and average permeability are 9.26% and 1.1523×10^{-3} μm^2, respectively. The main rock types include medium- to fine-grained feldspathic lithic sandstones and lithic sandstones: Chlorite rims, quartz enlargements, and weak dissolution of feldspar are commonly observed. Their mesopores are mostly primary intergranular pores and intragranular dissolution pores. These reservoirs can be classified as normal reservoirs.

For type III reservoirs, the average maximum mercury injection saturation is 82.27%, and the average mercury withdrawal efficiency is 36.19% (Table 1). This type of reservoir often has poor physical properties for gas production, and the average porosity and average permeability are 5.2% and 0.3517×10^{-3} μm^2, respectively. The major rock types are fine-grained feldspathic lithic sandstones, calcareous feldspathic lithic sandstones, and lithic sandstones. Because this type of reservoir contains abundant clay matrices and a low amount of quartz, the pores tend to get severely damaged during the compaction and diagenesis process. Furthermore, calcite cementation in some of the samples will lead to poorly developed pores. This type of reservoir is mainly composed of meso- and micropores, so type III reservoirs can be classified as poor reservoirs or non-reservoirs.

Fractal characteristics

According to fractal dimension calculations based on the capillary curves, a cross plot of lg(1-S_{Hg}) and lgPc can reveal the fractal characteristics of tight reservoirs (Lai et al. 2015). Usually, the value of the fractal dimension D is between 2 and 3, with a highly homogeneous pore structure having a D value of 2 and a highly heterogeneous pore structure having a D value of 3. We calculated the fractal dimension values for the samples from the Xu-6 member from our high-pressure mercury injection data. The calculated D values range between 2.42 and 2.81, with an average of 2.58. In detail, types I, II, and III reservoirs exhibit

different fractal characteristics, which correspond to pores of different sizes (Fig. 7 and Table 1). Type I reservoirs are dominated by macropores with a uniform distribution of meso- and micropores and fractal dimension values between 2.45 and 2.59. Type II reservoirs are dominated by mesopores and have fractal dimension values of 2.42–2.69. Type III reservoirs are dominated by micropores and fractal dimension values of 2.46–2.81.

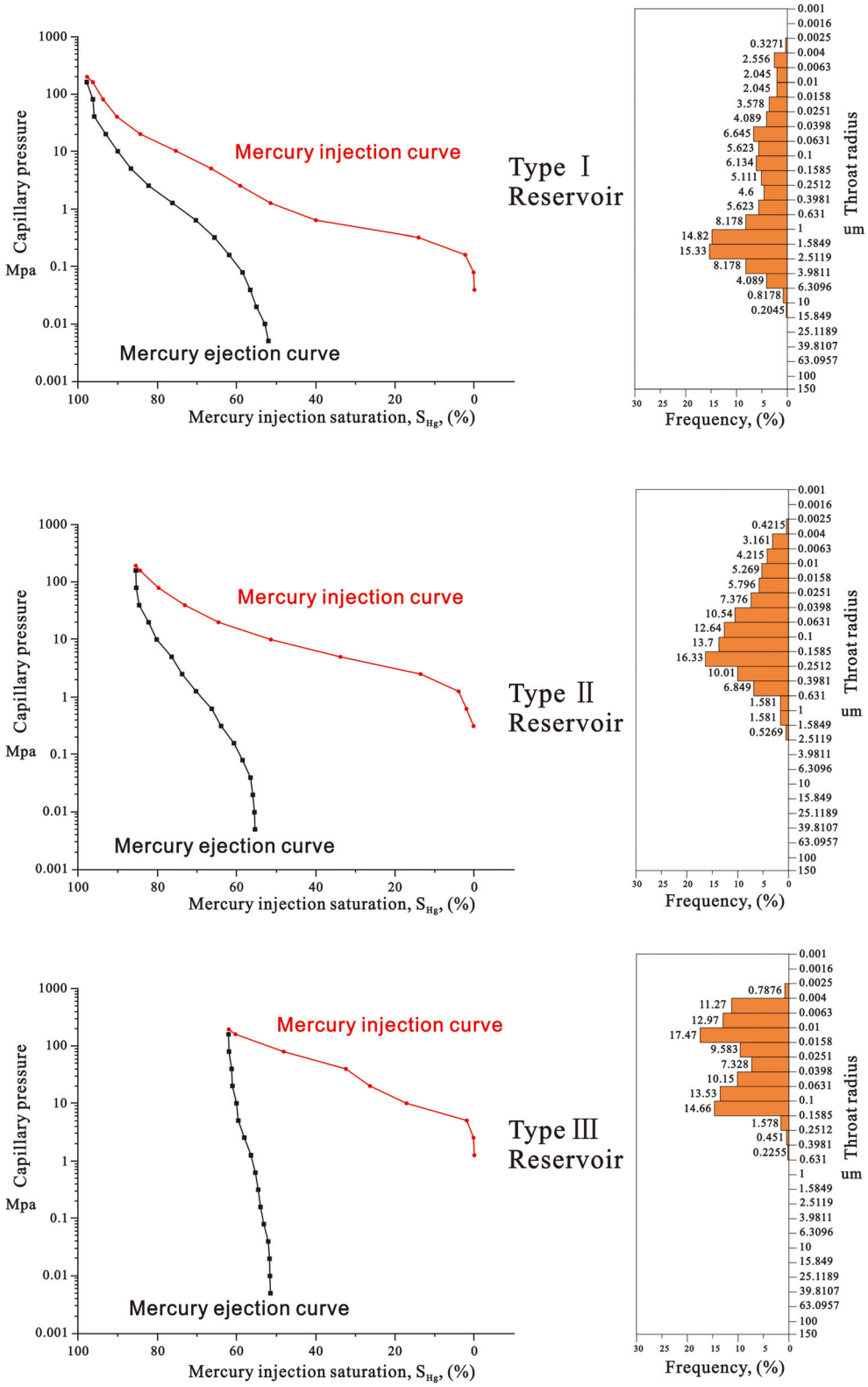

Fig. 6 Mercury pressure curves and pore throat radius distributions for different types of reservoirs of the Xu-6 member

Discussion

Vertical distribution and fractal characteristics of pores in reservoirs

As discussed in Lundegard (1992), compaction is the main factor responsible for reducing sandstone porosity. However, there is no linear relationship between sandstone porosity and effective vertical pressure, and the effects of other mechanical and geochemical mechanisms, such as the critical depth value, the ground temperature gradient, and secondary processes, need to be considered (Taylor et al. 2010). The Triassic Xujiahe Formation strata in Guang'an, Sichuan Basin, formed during a period of tectonic subsidence. The maximum burial depth during the Late Cretaceous was greater than 4000 m, and the ground temperature was higher than 150 °C. After this period, the burial depth gradually decreased to the current vertical depth of approximately 2100 m (Lai et al. 2018a; Zhao et al. 2010). Pores in the Xu-6 member of the Xujiahe Formation are mainly primary intergranular and intragranular dissolution pores (Lin et al. 2019). Specifically, the main interval in which macropores are dominant, mostly primary intergranular and mineral dissolution pores, lies within 2076–2085 m in vertical depth. The interval of mesopore dominance lies within 2042–2085 m. Tight sandstones that have experienced strong compaction or cementation (Zhang et al. 2019) and in which micropores are dominant lie within 2085–2090 m.

In the Xu-6 sandstones, the total pore volume and pore type are the dominant factors in determining the reservoir quality. As shown in Fig. 2, the sandstone samples with total pore volume greater than 1 cm^3 and dominated by macropores are considered type I high-quality reservoirs and are also the main gas-producing layers. Figure 8 shows that there is no significant overall correlation between the percentage of macropores and vertical depth; macropores dominantly appear only at distinct depth intervals. Xujiahe Formation sandstones experienced deep burial (> 4000 m) and then uplift, which likely compromised the linear relationship between porosity and depth at the initial stage (Taylor et al. 2010). Regarding the stratum level, as the vertical depth increases, porosity in reservoir sandstones shows an overall decreasing trend (Fig. 2), reflecting compaction by vertical pressure; however, some sandstone intervals in the deep section still show abundant macropores (Fig. 8), including intergranular dissolution pores formed by mineral dissolution and mechanical destruction pores formed by pressure-induced compaction. When reaching the critical depth of 2085 m, porosity sharply decreases, and micropores become the dominant pore type (Figs. 2 and 8A). In addition, the natural gamma (GR) curve of this section is characterized by a combined toothed bell shape, and the deep resistivity (RT) curve exhibits mostly low magnitudes; both curves show no distinct features for type I reservoirs (Fig. 2). It is noteworthy that the type I reservoirs

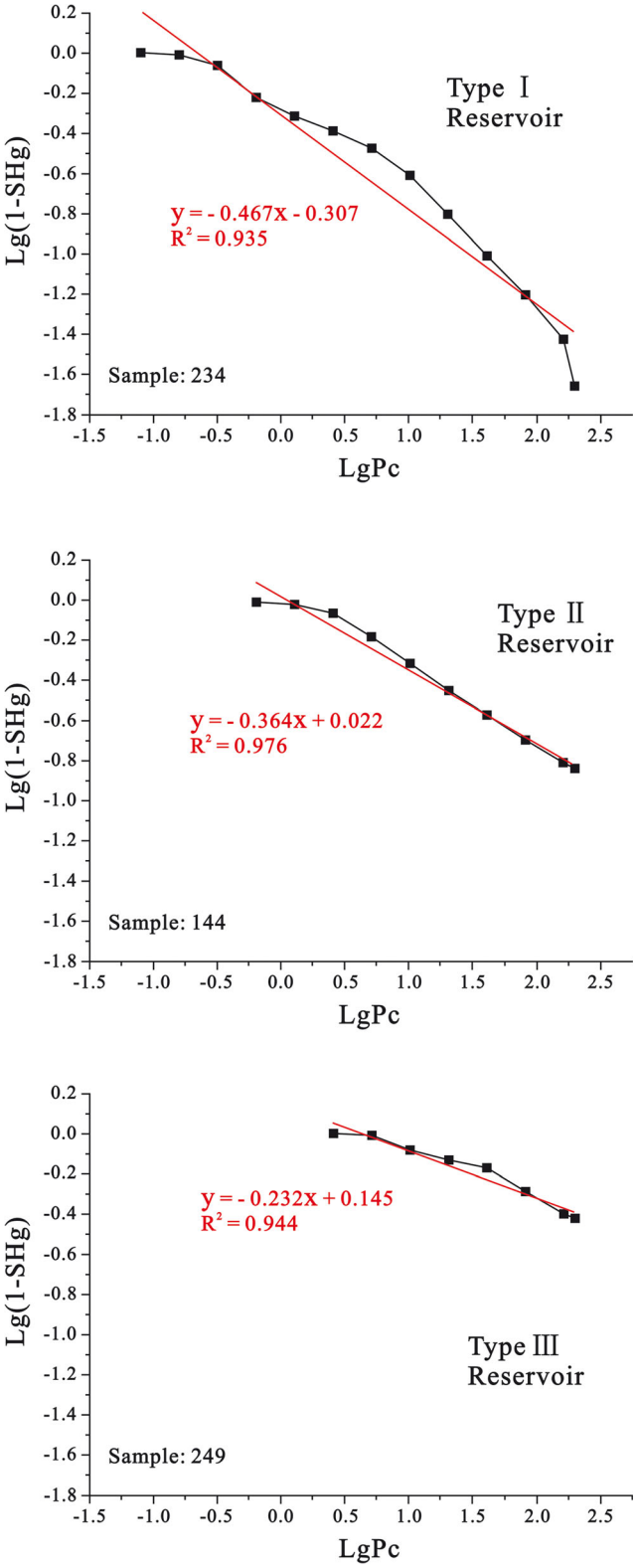

Fig. 7 Fractal characteristics of different reservoir types in the Xu-6 member

are characterized by generally large acoustic slowness values (AC) and low rock densities (DEN), and the combination of the curves of the two quantities appears as a box or bell shape

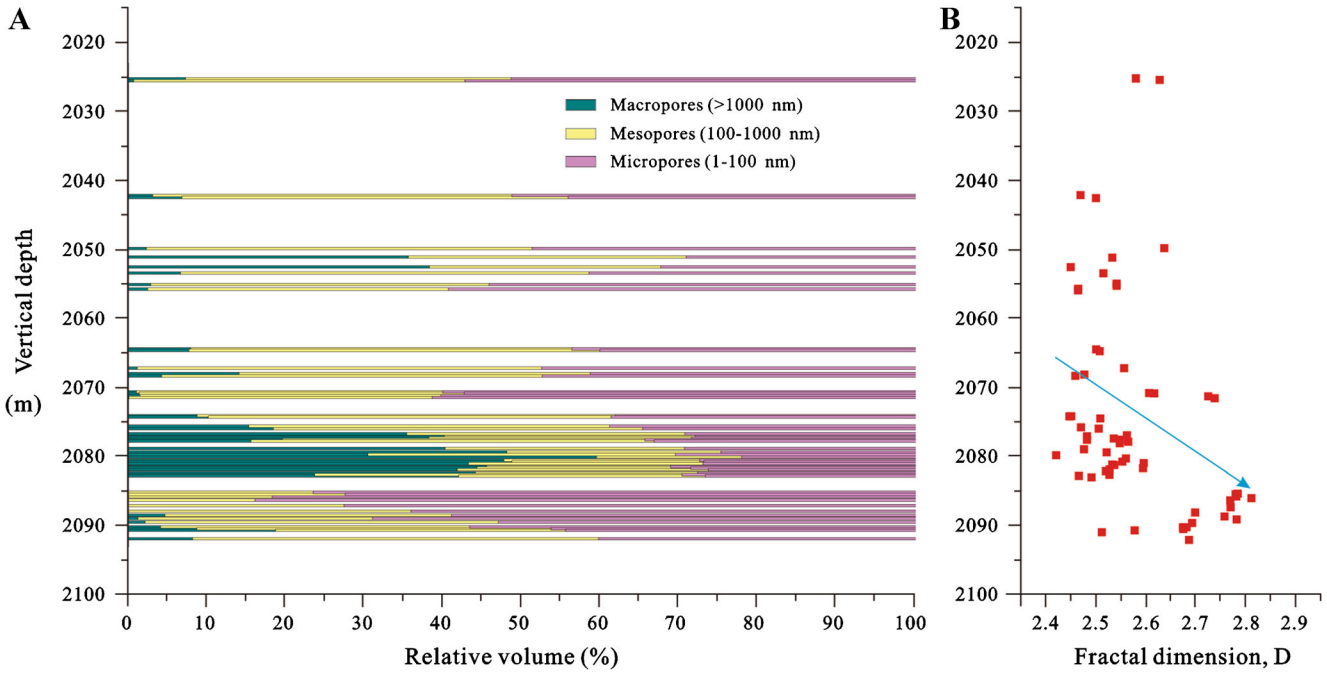

Fig. 8 Vertical variation in pore type and fractal dimension of gas reservoir sandstones in Guang'an well 101. **A** Relative volume (%). **B** Fractal dimension, *D*

(Fig. 2), revealing that this type of reservoir rock has large porosities and low densities.

Table 1 shows that the pore volume and type are the main factors in controlling the fractal dimension of the reservoir rocks. Pores in these two types of reservoirs are mainly macro- and mesopores, and their fractal dimensions lie between 2.45 and 2.6, with an average of 2.52 and 2.51 for types I and II, respectively. Therefore, it is difficult to distinguish between these two types of reservoirs solely based on the fractal dimension value; additional assistance is needed from the total pore volume and the mercury injection curve. In contrast, type III reservoirs are mostly composed of micropores, with fractal dimension values of 2.45–2.81 (2.67 on average). These sandstones, dominated by micropores, are characterized by strong heterogeneities, and they significantly differ from the other two types of reservoir sandstones. A few of the samples have fractal dimension values below 2.6, which is mainly caused by well-developed mesopores, the relative abundance of which is close to that of micropores. In brief, the fractal dimension value is obviously coupled with the pore types of tight sandstone (Fig. 8B) and can reflect its reservoir properties and percolation features. Hence, for effective prediction, exploration, and development of high-quality reservoirs, it is necessary to evaluate changes in reservoir microcharacteristics, such as the fractal dimension.

Physical properties and fractal dimension

The fractal dimension can be used as a parameter to represent the simple-complex degree and the homogeneous-heterogeneous

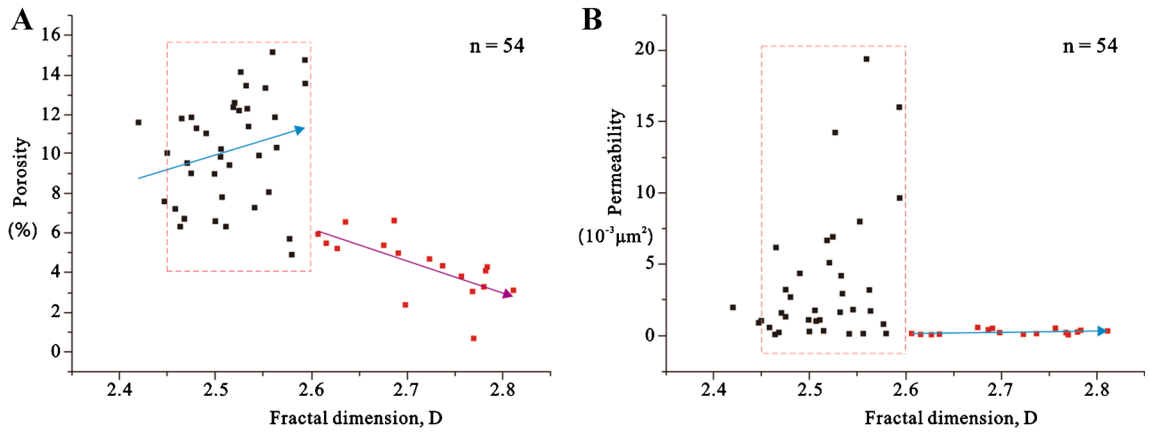

Fig. 9 Relationships between the fractal dimension and **A** porosity or **B** permeability in Xu-6 member sandstones

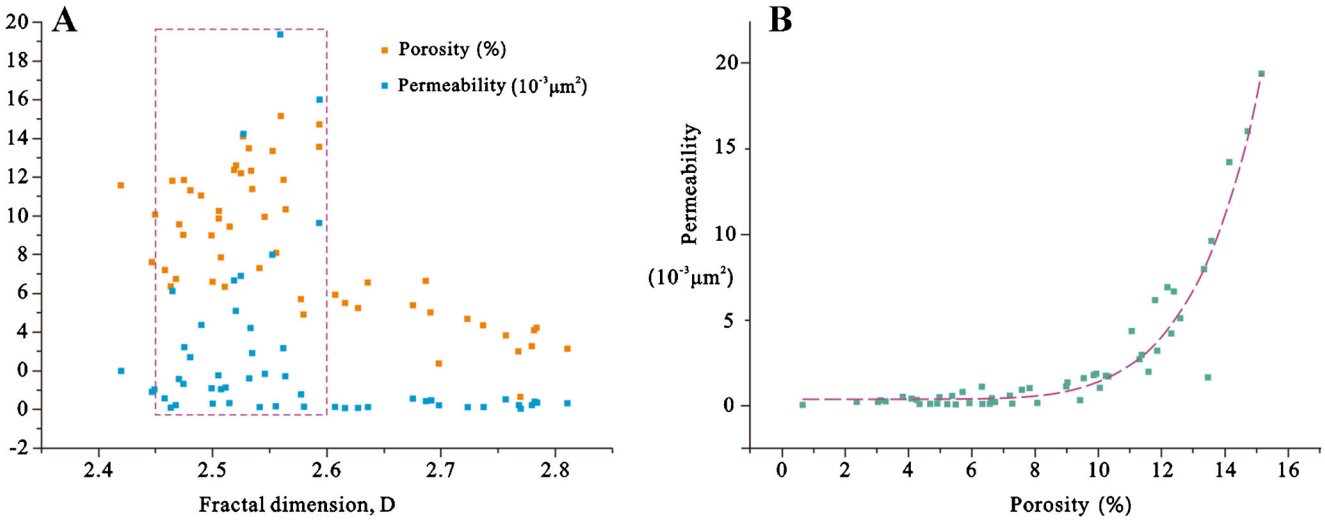

Fig. 10 Fig. 10 **A** Fractal dimension corresponds with porosity and permeabiltiy. **B** The relationship between porosity and permeability

property of sandstone pores, which can then be related to the sandstone porosity and permeability coefficient. Porosity in the Xu-6 reservoir sandstones varies significantly, ranging from 0.66 to 15.16%, with an average value of 7.45%. The porosity is related to the fractal dimension, with two different relationships separated by a critical value of 2.6. When the fractal dimension is smaller than 2.6, the sandstone porosity is relatively variable and shows a slight tendency towards higher values with increasing fractal dimension; when the fractal dimension is greater than 2.6, variation in porosity decrease and there is a distinct negative correlation between the two variables (Fig. 9A). Based on the observed relationship between sandstone porosity and fractal dimension, under the controlling effect of macro- and mesopores, there is a lot of variability and some increasing tendency below 2.6; in contrast, reservoir sandstones controlled by micropores show stronger heterogeneities, as supported by the trend of decreasing porosity with increasing fractal dimension above 2.6. Overall, it can be seen that the Xu-6 member sandstone has a clear fractal critical threshold: a fractal dimension value between 2.45 and 2.6 is the prerequisite for judging a tight sandstone to be a high-quality reservoir.

Previous studies have shown that reservoirs dominated by microscopic fractures and macropores possess a good connectivity and large permeability, which is advantageous for transporting and storing natural gas (Zhao ZW et al. 2019), and that reservoirs dominated by micropores become more irregular and complex due to alterations caused by compaction and diagenesis, which weakens the porosity and seepage capability of tight reservoir strata and adversely affects gas/fluid transport (Zeng 2010). In addition to pores, the complexity of clastic rocks in terms of their composition and grain shape also controls the fractal dimension of tight sandstones. The permeability of Xu-6 sandstones is within 0.0394–19.3679 × 10^{-3} μm² with an average value of 0.1582 × 10^{-3} μm². When plotting the sandstone permeability versus its fractal dimension, no obvious correlation is observed for homogenous-weakly heterogeneous sandstones($D \leq 2.6$); however, when the fractal dimension is greater than 2.6, the permeability of strongly heterogeneous sandstone is generally smaller than 0.5 × 10^{-3} μm² (Fig. 9B). In other words, strongly heterogeneous sandstones are dominated by micropores, which greatly decrease the permeability (to values close to 0).

Our statistical analyses of the Xu-6 sandstones in the Xujiahe Formation in Guang'an show that the fractal dimension values for the type I and II reservoir sandstones mainly range between 2.45 and 2.6, corresponding to a high level of porosity and permeability (Fig. 9 and 10A). In comparison, type III reservoir sandstones are affected by mechanical compaction and secondary cementation, resulting in reductions in the total pore volume, porosity, and permeability coefficient, which is reflected by their strong heterogeneities, as proxied by the > 2.6 fractal dimension. In our gas reservoir samples, the fractal dimension increases as the burial depth and clastic rock content increase. A larger burial depth represents a stronger compaction effect, which can reduce the total pore volume and porosity and consequently increase the heterogeneity.

Based on the microscopic characteristics of the thin sections, the pores in the Xu-6 sandstones are dominated by primary intergranular and secondary dissolution pores, with the rare occurrence of (microscopic) fractures. Thus, their storage capability is mainly determined by the pore structure. In this study, the gas reservoir sandstone samples exhibit a strong correlation between porosity and permeability: as porosity increases, permeability increases exponentially (Fig. 10B). As a pore-type reservoir, Xu-6 tight sandstones possess macropores that are well connected and are gradually replaced by meso- and micropores. The porosity is thus gradually enhanced (Fig. 10B), which, combined with erosion in the process of compaction, leads to the exponentially enlarged permeability of tight sandstones. In contrast, multiple Xujiahe Formation samples from

multiple wells have been shown to exhibit a linear correlation between porosity and permeability (Lai et al. 2018a). We suggest that the investigation of a single well can more precisely represent the coupling relationship between different physical properties in distinct areas of the gas reservoir, whereas overlaying of data from multiple wells from different studies holds the danger of generalized and ambiguous conclusions due to significant spatial heterogeneities.

Conclusion

Based on our microscopic observations of tight sandstone samples from well 101 in the Guang'an gas reservoir, statistical analyses of the rock samples, mercury injection tests, and calculations based on fractal theory, the following conclusions were obtained.

(1) The Xu-6 tight sandstones in the Xujiahe Formation can be divided into three reservoir types: type I reservoirs dominated by macro- and mesopores, type II reservoirs dominated by mesopores, and type III reservoirs dominated by meso- and micropores. Type I reservoirs are premier reservoirs and are characterized by pore volumes greater than 1 cm^3, porosities larger than 10%, permeability coefficients larger than 1.0×10^{-3} μm^2, and fractal dimension values of 2.45–2.6. In addition, these types of gas reservoir section exhibits larger acoustic slowness values and low rock densities, and the combination of the two corresponding curves appears as a box or bell shape.

(2) The varying distributions of pore types result in significant changes in the pore heterogeneity of different types of reservoirs, and strongly heterogeneous tight sandstones adversely affect the storage and transport of natural gas. The porosity and permeability of tight sandstones are dependent on the pore structure. When the fractal dimension is between 2.45 and 2.6, the sandstone porosity is high and variable with a tendency toward higher values with increasing fractal dimension, while the permeability is not correlated with the fractal dimension. When the fractal dimension is above 2.6, the porosity and the fractal dimension sharply drop and become negatively correlated, while permeability decreases to uniformly low values. In addition, as the burial depth increases, the fractal dimension also gradually increases, and the heterogeneity of sandstones is strengthened. As porosity increases, the permeability increases exponentially.

Funding This work was supported by the Special Project of Deep Resource Exploration of the National Key Research and Development Program of China (No. 2018YFC0604201) and the Open Fund of State Key Laboratory of Oil and Gas Reservoir Geology and Exploitation (Chengdu University of Technology) (No. PLC201901013).

Declarations

Conflict of interest The authors declare that they have no competing interests.

References

Albrecht D, Reitenbach V (2015) Investigations on fluid transport properties in the North-German Rotliegend tight gas sandstones and applications. Environ Earth Sci 73:5791–5799. https://doi.org/10.1007/s12665-015-4322-x

Chen G, Lin LB, Wang W, Chen HD, Guo TL (2014) Diagenesis and porosity evolution of sandstones in Xujiahe Formation, Yuanba area. Pet Geol Exp 36(4):405–410 (in Chinese with English abstract)

Deng T, Li Y, Wang ZJ, Yu Q, Hu WC, Zhao SZ, Dong SL (2018) The difference of pore structures and fractal features in the Xujiahe Formation shales from Well LD-1, Sichuan Basin, China. J Chengdu Univ Technol (SciTechnol Ed) 45(6):709–721 (in Chinese with English abstract)

Ehrenberg SN, Nadeau PH (2005) Sandstone vs. carbonate petroleum reservoirs: a global perspective on porosity-depth and porosity-permeability relationships. AAPG Bull 89:435–445. https://doi.org/10.1306/11230404071

Ehrenberg SN, Nadeau PH, Steen Ø (2009) Petroleum reservoir porosity versus depth: Influence of geological age. AAPG Bull 93:1281–1296. https://doi.org/10.1306/06120908163

Feng XZ, Zhu HH (2019) Micro-pore structure and fractal characteristics of the Xiashihezi Formation tight sandstone reservoirs in Sulige Area, Ordos Basin. Geol Sci Technol Inform 38(3):147–156 (in Chinese with English abstract)

Fu X, Wang ZH, Zhong B, Feng X, Li N (2010) Characteristics of single phase gas seepage in sandstone gas reservoirs with low-permeability and high water saturation in the sixth member of the Xujiahe Formation, Guang'an Gas Field. Nat Gas Ind 30(07):39–41+130 (in Chinese with English abstract)

Gu ZY (2017) Influences of diagenesis evolution difference on the Xu-2 and Xu-6 reservoir in the Dongfengchang area, southern Sichuan, China. J Chengdu Univ Technol (SciTechnol Ed) 44(02):139–148 (in Chinese with English abstract)

Hou Z, Xie H, Zhou H, Were P, Kolditz O (2015) Unconventional gas resources in China. Environ Earth Sci 73:5785–5789. https://doi.org/10.1007/s12665-015-4393-8

Huang JL, Dong DZ, Li JZ, Hu JW, Wang YM, Li DH, Wang SF (2016) Reservoir characteristics and its influence on continental shales: an example from Triassic Xujiahe Formation shale, Sichuan Basin. Earth Sci Front 23(2):158–166 (in Chinese with English abstract)

Huang W, Lu S, Hersi OS, Wang M, Deng S, Lu R (2017) Reservoir spaces in tight sandstones: classification, fractal characters, and heterogeneity. J Nat Gas Sci Eng 46:80–92. https://doi.org/10.1016/j.jngse.2017.07.006

Lai J, Wang G, Ran Y, Zhou Z (2015) Predictive distribution of high-quality reservoirs of tight gas sandstones by linking diagenesis to depositional facies: evidence from Xu-2 sandstones in the Penglai area of the central Sichuan basin, China. J Nat Gas Sci Eng 23:97–111. https://doi.org/10.1016/j.jngse.2015.01.026

Lai J, Wang G, Cai C, Fan Z, Wang S, Chen J, Luo G (2018a) Diagenesis and reservoir quality in tight gas sandstones: the fourth member of the Upper Triassic Xujiahe Formation, Central Sichuan Basin, Southwest China. Geol J 53:629–646. https://doi.org/10.1002/gj.2917

Lai J, Wang G, Wang S, Cao J, Li M, Pang X, Zhou Z, Fan X, Dai Q, Yang L, He Z, Qin Z (2018b) Review of diagenetic facies in tight sandstones: diagenesis, diagenetic minerals, and prediction via well

logs. Earth Sci Rev 185:234–258. https://doi.org/10.1016/j.earscirev.2018.06.009

Law BE, Curtis JB (2002) Introduction to unconventional petroleum systems. AAPG Bull 86:1851–1852. https://doi.org/10.1306/61EEDDA0-173E-11D7-8645000102C1865D

Li Y, Chen SJ, Wu BY, Qiu D, Lin RP, Li JL (2017) Controlling factors on complex gas-water distribution in Xu-6 tight sandstone gas reservoir in Guang'An area. Xinjiang Petrol Geol 38(02):198–203 (in Chinese with English abstract)

Lin XB, Tian JC, Liu LP, Li MT (2019) Dissolution mechanism of siliciclastic particles in Xujiahe Formation, West Sichuan Depression, Sichuan Basin. Pet Geol Exp 41(3):404–410 (in Chinese with English abstract)

Lundegard PD (1992) Sandstone porosity loss; a big picture view of the importance of compaction. J Sediment Res 62:250–260. https://doi.org/10.1306/D42678D4-2B26-11D7-8648000102C1865D

Luo C, Jia AL, He DB, Guo JL, Zhang G, Cheng ZJ (2016) A new method for binomial deliverability equation of horizontal gas well. Nat Gas Geosci 27(02):359–370 +376 (in Chinese with English abstract)

Nelson PH (2009) Pore-throat sizes in sandstones, tight sandstones, and shales. AAPG Bull 93:329–340. https://doi.org/10.1306/10240808059

Paxton ST, Szabo JO, Ajdukiewicz JM, Klimentidis RE (2002) Construction of an intergranular volume compaction curve for evaluating and predicting compaction and porosity loss in rigid-grain sandstone reservoirs. AAPG Bull 86:2047–2067. https://doi.org/10.1306/61EEDDFA-173E-11D7-8645000102C1865D

Pittman ED, Larese RE (1991) Compaction of lithic sands: experimental results and applications (1). AAPG Bull 75:1279–1299

Schmoker JW (2002) Resource-assessment perspectives for unconventional gas systems. AAPG Bull 86:1993–1999. https://doi.org/10.1306/61EEDDDC-173E-11D7-8645000102C1865D

Shi ZS, Xie WR, Ma SY, Li GX (2012) Transgression sedimentary records of the Members 4-6 of Upper Triassic Xujiahe Formation in Sichuan Basin. J Palaeogeogr 14(05):583–595

Taylor TR, Giles MR, Hathon LA, Diggs TN, Braunsdorf NR, Birbiglia GV, Kittridge MG, Macaulay CI, Espejo IS (2010) Sandstone diagenesis and reservoir quality prediction: models, myths, and reality. AAPG Bull 94:1093–1132. https://doi.org/10.1306/04211009123

Tong CG (2000) Relationship between Neotectonic movement and structural evolution and gas pools formation of Sichuan Basin. J Chengdu Univ Technol (SciTechnol Ed) 27(02):123–130 (in Chinese with English abstract)

Wang Z, Huang S, Gong D, Wu W, Yu C (2013) Geochemical characteristics of natural gases in the Upper Triassic Xujiahe Formation in the southern Sichuan Basin, SW China. Int J Coal Geol 120:15–23. https://doi.org/10.1016/j.coal.2013.09.002

Yu C, Gong DY, Huang SP, Wu W, Liao FR, Liu D (2014) Geochemical characteristics of carbon and hydrogen isotopes for the Xujiahe Formation natural gas in Sichuan Basin. Nat Gas Geosci 25(1):87–97

Zeng L (2010) Microfracturing in the Upper Triassic Sichuan Basin tight-gas sandstones: tectonic, overpressure, and diagenetic origins. AAPG Bull 94:1811–1825. https://doi.org/10.1306/06301009191

Zhang L, Wang W, Shu ZG, Hao F, Zou YH, Yang S (2019) Distribution and genesis of calcite-replaced and calcite-cemented tight reservoirs in Xujiahe Formation, Yuanba area, Northeast Sichuan. Acta Pet Sin 40(6):692–705 (in Chinese with English abstract)

Zhao W, Wang H, Xu C, Bian C, Wang Z, Gao X (2010) Reservoir-forming mechanism and enrichment conditions of the extensive Xujiahe Formation gas reservoirs, central Sichuan Basin. Pet Explor Dev 37:146–157. https://doi.org/10.1016/S1876-3804(10)60022-5

Zhao ZW, Li N, Liu M, Wang XJ, Wu CJ, Li L (2019) Origin of gas accumulation and high yield in tight gas reservoirs of Xujiahe Formation, Sichuan Basin. Nat Gas Explor Develop 42(2):39–47 (in Chinese with English abstract)

Zhao XF, Zhao TY, Zhang WL (2019) An introduction to the developments of tidal rhythmite studies and its implication to the natural gas exploration of Xujiahe Formation. Nat Gas Explor Develop 42(2):29–38 (in Chinese with English abstract)

Zheng RC, Dai CC, Zhu RK (2009) Sequence-based lithofacies and paleogeographic characteristics of Upper Triassic Xujiahe Formation in Sichuan Basin. Geol Rev 55(4):484–495 (in Chinese with English abstract)

Zhu T, Duan XG, He D, Peng X (2014) Reservoir characteristics in the 6th Member of Xujiahe Formation in Guang'an area of Sichuan Province. Journal of Yangtze University(Nat Sci Edit), 11(26): 5–7+35+3. (in Chinese with English abstract)

Zhu HH, Zhong DK, Zhang YX, Sun HT, Du BQ, Meng H, Zhang CW, Yang Z (2014) Pore types and controlling factors on porosity and permeability of Upper Triassic Xujiahe tight sandstone reservoir in Southern Sichuan Basin. OIL Gas Geol 35(1):65–76 (in Chinese with English abstract)

Zhu F, Hu W, Cao J, Sun F, Liu Y, Sun Z (2018) Micro/nanoscale pore structure and fractal characteristics of tight gas sandstone: a case study from the Yuanba area, northeast Sichuan Basin, China. Mar Pet Geol 98:116–132. https://doi.org/10.1016/j.marpetgeo.2018.08.013

Zhu H, Zhang T, Zhong D, Li Y, Zhang J, Chen X (2019) Binary pore structure characteristics of tight sandstone reservoirs. Pet Explor Dev 46:1297–1306. https://doi.org/10.1016/S1876-3804(19)60283-1

Zou C, Tao S, Zhu R, Yuan X, Li W, Guangya Z, Xiangxiang Z, Xiaohui G, Liuhong L, Chunchun X, Jiarong S, Guohui L (2009) Formation and distribution of "continuous" gas reservoirs nd their giant gas province: a case from the Upper riassic Xujiahe Formation giant gas province, Sichuan Basin. Pet Explor Dev 36:307–319. https://doi.org/10.1016/S1876-3804(09)60128-2

Zou C, Zhu R, Liu K, Su L, Bai B, Zhang X, Yuan X, Wang J (2012) Tight gas sandstone reservoirs in China: characteristics and recognition criteria. J Pet Sci Eng 88–89:82–91. https://doi.org/10.1016/j.petrol.2012.02.001

Zou CN, Yang Z, Tao SZ, Yuan XJ, Zhu RK, Hou LH, Wu ST, Sun L, Zhang GS, Bai B, Wang L, Gao XH, Pang ZL (2013) Continuous hydrocarbon accumulation over a large area as a distinguishing characteristic of unconventional petroleum: the Ordos Basin, North-Central China. Earth Sci Rev 126:358–369. https://doi.org/10.1016/j.earscirev.2013.08.006

Zou CN, Yang Z, Zhu RK, Zhang GS, Hou LH, Wu ST, Tao SZ, Yuan XJ, Dong DZ, Wang YM, Wang L, Huang JL, Wang SF (2015) Progress in China's unconventional oil&gas exploration and development and theoretical technologies. Acta Geol Sin 89(06):979–1007 (in Chinese with English abstract)